

Time-dependent Electronic Populations in Fragment-based Time-dependent Density Functional Theory

Martín A. Mosquera^{1*}, Adam Wasserman^{1,2}

¹Department of Chemistry
Purdue University, 560 Oval Drive, West Lafayette, IN 47907, USA

²Department of Physics and Astronomy
Purdue University, 525 Northwestern Avenue, West Lafayette, IN 47907, USA

awasser@purdue.edu

April, 2015

Abstract

Conceiving a molecule as composed of smaller molecular fragments, or subunits, is one of the pillars of the chemical and physical sciences, and leads to productive methods in quantum chemistry. Using a fragmentation scheme, efficient algorithms can be proposed to address problems in the description of chemical bond formation and breaking. We present a formally exact time-dependent density-functional theory for the electronic dynamics of molecular fragments with variable number of electrons. This new formalism is an extension of previous work [Phys. Rev. Lett. **111**, 023001 (2013)]. We also introduce a stable density-inversion method that is applicable to time-dependent and ground-state density-functional theory, and their extensions, including those discussed in this work.

1 Introduction

Simple and productive methods to investigate dynamical features of solids and molecules are offered by Time-dependent Density-functional Theory (TDDFT) [1]. TDDFT embodies many concepts and formal exact results, but its core is the 1-1 correspondence [2] between time-dependent (TD) external potentials and TD electronic densities, provided the initial state of the system is given. Every observable of the system is expressed as a TD density-functional. The calculation of the density is carried out by solving the TD Kohn-Sham (KS) equations [3], which are single-particle Schrödinger equations that require an approximation to the exchange-correlation (XC) potential, a density-functional.

The adiabatic local density approximation (ALDA) [4] to the TD XC potential is the simplest, useful approximation to study the dynamics of atoms and solids. However, when applied to molecules, ALDA often yields unphysical results, for example, atoms with fractional charges at dissociation, under-

estimated charge-transfer excitation energies, missing double excitations, among others. Two decades of research have shown that it is challenging to enhance the performance of ALDA while preserving computational simplicity and elegance.

The TD KS equations describe all of the electrons as part of a single entity, imposing a limit on the number of atoms that can be simulated in a reasonable amount of time. This limit can be increased by dividing a molecule into fragments and performing inexpensive calculations on each individual fragment. Several approximated methods to investigate the electron dynamics of molecules as composed of fragments are available [5–8]. These methods typically assign a set of TD single-particle Schrödinger equations (not necessarily TD KS equations) to every fragment in the molecule. The fragment electrons are subject to the usual interactions as if they were in the presence of the fragment nuclei only; and, an extra potential, usually fragment-dependent, accounting for the interaction between the fragments, is added. Successful applications to the calculation of solvachromatic shifts [9, 10] and excitation energy of monomers [6] have been reported.

*Present address: Department of Chemistry, Northwestern University, 2145 Sheridan Road, Evanston, IL 60208, USA

A rigorous extension of TDDFT for molecules made of chemical fragments was presented in Ref. [11]. In this extension, a molecule is divided into fragments, each a set of atoms. Every fragment is assigned an initial state, and a Hamiltonian including a global, auxiliary potential, termed partition potential, which enforces that the total electronic density is the true TD electronic density of the molecule. We proved that the partition potential is uniquely determined by the TD electronic density of the system, and that it can thus be expressed (and approximated) as a density-functional. The linear response and an extension to consider electromagnetic fields are presented in Ref. [12]. The Hamiltonians used in Refs. [11] and [12], and the aforementioned approximated methods, are particle-conserving, i.e., the average number of electrons in a fragment is time-independent; this restriction is eliminated in this work.

In this paper we first introduce a density-inversion method that improves that of Ref. [11] and allows us to estimate the partition potential. Using a model for the errors, we discuss, in close connection with standard TDDFT, the origin of uncertainties of the partition potential in regions far from the molecule. We extend our fragment-based TDDFT [11] to allow for variable numbers of electrons in each fragment, while preserving the uniqueness of observables as density-functionals. The formalism introduced in this paper serves as a theoretical foundation for the development of methods accounting for electronic excitations and electron-transfer processes, without sacrificing explicit use of the electronic density and computational efficiency.

2 Fragment-based TDDFT

2.1 Formulation

An electron in a fragment, labeled α , is subject to a 1-body external potential, denoted as v_α . For example, $v_\alpha(\mathbf{r}) = \sum_{i \in I_\alpha} -Z_i/|\mathbf{r} - \mathbf{R}_i|$; I_α is a set of labels for the nuclei in fragment α . We assign to each fragment in the molecule a Hamiltonian that includes an auxiliary potential, the partition potential v_p :

$$\hat{H}_\alpha[v_p](t) = \hat{H}_\alpha^0 + \int d^3\mathbf{r} \hat{n}(\mathbf{r})v_p(\mathbf{r}) , \quad (1)$$

where $\hat{H}_\alpha^0 = \hat{T} + \hat{W} + \int d^3\mathbf{r} \hat{n}(\mathbf{r})v_\alpha(\mathbf{r})$, \hat{T} and \hat{W} are the kinetic, and coulombic repulsion energy operators, respectively, and $\hat{n}(\mathbf{r})$ is the density operator. This Hamiltonian does not include external driving

forces other than those due to the nuclei of fragment α . TD displacement of the positions of the nuclei can be described by introducing a time-dependent Hamiltonian where v_α is replaced by the corresponding TD fragment-potential, $\sum_{i \in I_\alpha} -Z_i/|\mathbf{r} - \mathbf{R}_i(t)|$.

The state of a fragment is described by the evolution of the ket $|\psi_\alpha[v_p](t)\rangle$ in Fock space, which satisfies the TD Schrödinger equation (atomic units are used throughout):

$$i\partial_t|\psi_\alpha[v_p](t)\rangle = \hat{H}_\alpha[v_p](t)|\psi_\alpha[v_p](t)\rangle , \quad (2)$$

where

$$|\psi_\alpha(t)\rangle = \sum_M \nu_{\alpha,M}|\psi_{\alpha,M}(t)\rangle . \quad (3)$$

$\{\psi_{\alpha,M}\}$ are kets corresponding to states with integer number of particles and $\{\nu_{\alpha,M}\}$ are the weight amplitudes of those states. Kets with different number of electrons are orthogonal, $\langle\psi_{\alpha,M}|\psi_{\alpha,M'}\rangle = 0$, $M \neq M'$. The total density is given as

$$n(\mathbf{r}t) = \sum_\alpha n_\alpha(\mathbf{r}t) , \quad (4)$$

which defines v_p when $n_\alpha(\mathbf{r}t) = \langle\psi_\alpha(t)|\hat{n}(\mathbf{r})|\psi_\alpha(t)\rangle$, as proven in Ref. [11]: Given a set $\{\psi_{\alpha,0}, v_\alpha\}$, two potentials v_p and v'_p that differ by more than a TD constant *cannot give rise to the same density*. A corollary of this theorem is that there is a TD density-functional that, when evaluated at a given TD electronic density, gives the corresponding TD partition potential¹.

The partition potential represents the TD electronic density of the supermolecule, and is decomposed as follows [12]:

$$v_p(\mathbf{r}t) = v_G(\mathbf{r}t) + v_d(\mathbf{r}t) . \quad (5)$$

v_G is a “gluing potential”, accounting for the correlation between the fragments, and v_d is the driving potential the molecule is subject to (e.g. laser field). The gluing potential yields the shape of the potential such that the TD electronic density is recovered. The gluing potential satisfies [12]:

$$\begin{aligned} \frac{1}{i}\nabla \cdot n(\mathbf{r}t)\nabla v_G(\mathbf{r}t) &= \langle\psi(t)|[\hat{H}^0, \nabla \cdot \hat{\mathbf{j}}(\mathbf{r})]|\psi(t)\rangle \\ &- \sum_\alpha \langle\psi_\alpha(t)|[\hat{H}_\alpha^0, \nabla \cdot \hat{\mathbf{j}}(\mathbf{r})]|\psi_\alpha(t)\rangle . \end{aligned} \quad (6)$$

¹This theorem and corollary were recently used in Ref. [13] to propose an inversion method in the context of embedding potential-functional theory.

The terms on the right-hand-side of Eq.(6) are TD density-functionals. Approximating these terms and solving the resulting differential equation yields an estimate of the gluing potential. Another route to approximating v_G is by assuming that the system evolves adiabatically from its ground states, driven by a very slowly-varying field. In such case, the potential v_G is obtained from the adiabatic approximation in ground-state Partition DFT [14, 15]:

$$v_G^{\text{Ad}}[n(t)] = v_p^{\text{Ad}}[n(t)] - v^{\text{HK}}[n(t)] , \quad (7)$$

where $v^{\text{HK}}[n(t)]$ is the external perturbation the interacting electrons are subject to in their ground-state in order to yield the density $n(\mathbf{r}t)$ (the uniqueness of v^{HK} follows from the Hohenberg-Kohn theorem). The partition potential, $v_p^{\text{Ad}}[n(t)]$, is the Lagrange multiplier required to solve the minimization:

$$\min_{\{\psi_\alpha\} \rightarrow n(t)} \sum_\alpha \langle \psi_\alpha | \hat{H}_\alpha^0 | \psi_\alpha \rangle . \quad (8)$$

under the constraint of Eq.(4). The Lagrange multiplier for this problem is unique, up to an arbitrary constant [16].

The TD partition KS equations are:

$$i\partial_t \phi_{i,\alpha}(\mathbf{r}, t) = \left(-\frac{1}{2} \nabla^2 + v_{\text{Hxc}}[n_\alpha](\mathbf{r}, t) + v_\alpha(\mathbf{r}) + v_G[n](\mathbf{r}, t) + v_d(\mathbf{r}, t) \right) \phi_{i,\alpha}(\mathbf{r}, t) . \quad (9)$$

The density can be obtained by means of: $n(\mathbf{r}, t) = \sum_{i\alpha} f_{i\alpha} |\phi_{i\alpha}(\mathbf{r}, t)|^2$, where $\{f_{i\alpha}\}$ are the (time-independent) occupation numbers, chosen from a proper ensemble [11].

3 Classical Interpretation of the Partition Potential

Consider a system composed of a single massive particle, and a bath made of particles much smaller than the massive one. All the particles in the particle+bath system interact via a potential, U_{int} , of the form $\sum_{i>j} u_{ij}(\mathbf{r}_i - \mathbf{r}_j)$. The evolution of the subsystem particle, labeled S, is dictated by Eq. (2). There is no partitioning of the external potential because the particle and the bath are subject, implicitly, to a macroscopic, external, confining potential. The Hamiltonian of the subsystem particle is thus $\hat{H}_S = \hat{T} + \int d^3\mathbf{r} \hat{n}(\mathbf{r})v_p(\mathbf{r}t)$, and the Hamiltonian of the bath is $\hat{H}_B = \hat{T} + \hat{W} + \int d^3\mathbf{r} \hat{n}(\mathbf{r})v_p(\mathbf{r}t)$. The average position of the particle is $\bar{\mathbf{r}}_S(t) = \int d^3\mathbf{r} \mathbf{r} n_S(\mathbf{r}, t)$, where $n_S(\mathbf{r}, t) = |\psi(\mathbf{r}, t)|^2$.

By the Ehrenfest theorem and correspondence principle we have

$$m_S \frac{d^2 \bar{\mathbf{r}}_S}{dt^2} = \mathbf{F}_{p,S}(t) , \quad (10)$$

where $\mathbf{F}_{p,S}(t) = -\int d^3\mathbf{r} n_S(\mathbf{r}, t) \nabla v_p(\mathbf{r}, t)$, and m_S is the mass of the particle. Comparison with the equation of motion of the real system indicates that, in the classical limit, $(\nabla v_p)(\bar{\mathbf{r}}_S(t)) = (\nabla_{\mathbf{r}_S} U_{\text{int}})(\bar{\mathbf{r}}_S(t), \bar{\mathbf{r}}_B(t))$, where $\bar{\mathbf{r}}_B$ is the average coordinate of the bath. The partition force at the position of the particle is simply the force exerted on the particle by the bath.

As the mass of the subsystem particle is increased, the density tends to a Dirac distribution. It follows from the above result and Eq. (6) that the shape of the partition potential for any point but that of the particles is indefinite. However, for given initial momenta and coordinates of the particles and bath (this condition replaces the requirement that the initial wavefunction be specified), the trajectory of the momenta of the total system is in a one-to-one correspondence with the trajectory of partition forces exerted on each particle. Furthermore, if the assumptions of Langevin dynamics are applicable, the partition force on the massive particle can be interpreted as $\mathbf{F}_{p,S}(t) = -\gamma \mathbf{v}_S(t) + \mathbf{F}_{\text{ran}}(t)$, where $\mathbf{v}_S(t) = d\bar{\mathbf{r}}_S/dt$, γ is the friction coefficient, and \mathbf{F}_{ran} is the random force.

The gradient of v_p can *only* be known at the position of the particles, nowhere else. In the original proof by Runge and Gross [2], and its extension for partition potentials [11], it was found that potentials whose gradients grow rapidly in regions distant from the molecule are not covered. This result, as illustrated in Section 4, is related to the uncertainty in the estimation of the partition potential near the boundaries of the simulation box.

4 Numerical TD Potentials

TDDFT, in which our formulation is built upon, concerns itself with the simplification of the problem:

$$(i\partial_t - \hat{H}^\lambda[v](t))|\psi(t)\rangle = 0, \quad |\psi(0)\rangle = |\psi_0\rangle , \quad (11)$$

where

$$\hat{H}^\lambda[v](t) = \hat{T} + \lambda \hat{W} + \int d^3\mathbf{r} \hat{n}(\mathbf{r})v(\mathbf{r}t) . \quad (12)$$

Runge and Gross [2] showed that if v is Taylor-expandable around $t = 0$ and does not have physical anomalies in the boundaries, then v determines n

uniquely up to a TD constant in the potential; this theorem (recently used to formulate quantum control in TDDFT [17]) can be extended to include non-analytic potentials [18]. Let us denote the RG map as $\Lambda_{\psi_0}^\lambda$; thus, $n(t) = \Lambda_{\psi_0}^\lambda[v](t)$. The operator \hat{W} can stand for different types of electron-electron interactions, such as screened coulombic repulsion. If $\lambda = 0$, then the electrons are non-interacting.

Suppose a well behaved density, n^{ref} , and an initial state, ψ_0 , are known. If v_1 and v_0 exist, where $v_\lambda(t) = (\Lambda_{\psi_0}^\lambda)^{-1}[n^{\text{ref}}](t)$, then the Hartree-exchange-correlation potential for the system, by definition, is $v_{\text{HXC}} = v_0 - v_1$. Using the exact map Λ_{ψ_0} would require solving the TD Schrödinger equation, which is what one wants to avoid in practical calculations.

For the development of functionals, exploration of the map $\Lambda_{\psi_0}^\lambda$ is fruitful; this map could be investigated by solving the problem $n^{\text{ref}}(t) - \Lambda_{\psi_0}^\lambda[v](t) = 0$, which is a root-finding problem. The first order response of the density for some perturbation δv is $\delta n(\mathbf{r}t) = \int d^3\mathbf{r}'t' \chi^{-1}(\mathbf{r}t, \mathbf{r}'t')\delta v(\mathbf{r}'t')$. The response function χ^{-1} should decay in the asymptotic regions because large perturbations of v in those regions have a small response in n . This relation between densities and potentials introduces instabilities in root-finding algorithms aimed at reproducing the density corresponding to a given external potential. In the ground-state case, the instabilities could be eliminated by enforcing satisfaction of eigenvalue constraints. For three dimensional applications, in general, capturing the asymptotic regions is difficult when Gaussian basis sets are used because they do not have the correct asymptotic behavior.

Instead of looking for the exact root, one can solve a minimization problem:

$$\min_{v \in \mathcal{V}} \int_0^T \|n^{\text{ref}}(s) - \Lambda_{\psi_0}^\lambda[v](s)\|^2 ds, \quad (13)$$

where $\|f\|$ is a suitable spatial norm, and \mathcal{V} is a space of physical potentials. The quantities $n^{\text{ref}}(t)$ and $\langle \psi[v](t) | \hat{n}(\mathbf{r}) | \psi[v](t) \rangle$ need to be approximated. Let us write $n^{\text{ref}}(t) - \Lambda_{\psi_0}^\lambda[v](t) = \tilde{n}^{\text{ref}}(t) - \tilde{\Lambda}_{\psi_0}^\lambda[v](t) + \epsilon[n^{\text{ref}}, v]$. $\tilde{n}^{\text{ref}}(t)$ is the approximation to $n^{\text{ref}}(t)$ and $\tilde{\Lambda}_{\psi_0}^\lambda[v]$ is the approximation to $\Lambda_{\psi_0}^\lambda$. If v^* is the exact potential representing n^{ref} , then the problem becomes $\tilde{n}^{\text{ref}} = \tilde{\Lambda}_{\psi_0}^\lambda[v^*] + \epsilon$. Because we cannot use exact methods to determine n^{ref} and $\Lambda_{\psi_0}^\lambda$, we assume that ϵ is a random function of the space-time coordinates. Moreover, one would expect that \tilde{n}^{ref} and $\tilde{\Lambda}_{\psi_0}^\lambda$ have smooth timespace gradients, and that ϵ displays

autocorrelation because the spacing between points is arbitrarily small.

4.1 Estimation of the Partition Potential

Let \mathcal{V}_p be a space of TD partition potentials, and \mathcal{D} a space of TD densities and define the map:

$$\Lambda_{S_0} : \mathcal{V}_p \rightarrow \mathcal{D}, \quad (14)$$

where $S_0 = \{\psi_{\alpha,0}, v_\alpha\}$. For a given TD partition potential, the density is obtained by evaluation of the above map at the given partition potential; in other words, $n(t) = \Lambda_{S_0}[v_p](t)$. This map depends on the history of the partition potential, i.e., it has memory dependence [11].

Let v_p^* be the true partition potential. We assume that, due to numerical errors, the estimation to the reference density \tilde{n}^{ref} is of the form $\tilde{n}^{\text{ref}} = \tilde{\Lambda}_{S_0} + \epsilon$, where ϵ is a *random function*. To estimate the partition potential corresponding to \tilde{n}^{ref} we minimize:

$$\|e[v_p]\|_\mu^2 = \|\tilde{n}^{\text{ref}} - \tilde{\Lambda}_{S_0}[v_p]\|_\mu^2, \quad (15)$$

where $d\mu(\mathbf{r}, t)$ is the measure.

Since ϵ is a function, its probability density function (PDF) is a *functional*. The PDF depends on parameters, denoted collectively as Θ , and the PDF itself as $D([\epsilon]|\Theta)$. The probability that ϵ is observed in a set \mathcal{U} is given by the path integral:

$$P(\epsilon \in \mathcal{U}|\Theta) = \int_{\mathcal{U}} dm_L[\epsilon] D([\epsilon]|\Theta), \quad (16)$$

where the measure over the space of errors is m_L . The traditional methods of non-linear regression can be applied to estimate the best parameters of the distribution, Θ^* , for a given set of observations. Then a Taylor expansion in terms of the parameters can be used to generate their PDF, which can then be used to estimate the error in the parameters. In this case, the parameters are the variance and the partition potential.

In the next section, we will expand the partition potential in a spline basis set. The parameters are the values of the partition potential at the knots, and they are correlated: A perturbation of the partition potential at one knot affects the response of the density in other knots. Hence, we must employ a model of correlated errors. Finding the correct model is a demanding task beyond the scope of this work. For this reason, we choose a biased model based on the

following observations: i) A measure of the error of the form $\int d^3\mathbf{r}dt (\tilde{n}^{\text{ref}}(\mathbf{r}, t) - \tilde{\Lambda}_{S_0}[v_p])^2$ suffers of autocorrelation. ii) Far from the molecule, the partition potential has little influence on the density. iii) Estimating the density is not sufficient; its spatio-temporal gradient is an important quantity. An error measure accounting for these observations is:

$$\|e[v_p]\|_{\mu}^2 = \int d\mu(\mathbf{r}, t) \{ |\nabla e(\mathbf{r}, t)|^2 + (\partial_t e(\mathbf{r}, t))^2 \}. \quad (17)$$

Based on ii), we choose a measure of the form $d\mu(\mathbf{r}, t) = d^3\mathbf{r}dt \sum_i \tilde{n}^{\text{ref}}(\mathbf{r}_i, t) \delta(\mathbf{r} - \mathbf{r}_i)$. Where $\{\mathbf{r}_i\}$ are points selected in such a way that $|\nabla e|^2 + (\partial_t e)^2$ resembles a χ^2 -distribution. To apply this measure of error in the next section, we transform the above measure into a vector norm. Then, the resultant distribution is expanded in terms of the partition potential evaluated at the knots, and asymptotic analysis is applied [19], leading to the random variables required to reproduce the density within a small error tolerance.

4.2 1d Electron in a Double-well Potential

Let us revisit the example considered in Ref. [11]: A one dimensional “electron” in a double well potential. The TD partition equations are:

$$i\partial_t \phi_{\alpha}(x, t) = \left(-\frac{1}{2}\partial_x^2 + v_{\alpha}(x) + v_p(x, t) \right) \phi_{\alpha}(x, t), \quad (18)$$

where $\alpha = L, R$, standing for left and right wells. The potentials are $v_{\alpha}(x) = v_0/\sqrt{(x - x_{\alpha})^2 + a}$; the parameters are: $v_0 = -1$, $x_R - x_L = 4$, and $a = 1$. The density is obtained by averaging over the orbital densities of both wells:

$$n(x, t) = \frac{1}{2}|\phi_L(x, t)|^2 + \frac{1}{2}|\phi_R(x, t)|^2. \quad (19)$$

Suppose that the supermolecule evolves from the ground state driven by a monochromatic laser. The evolution of the system is thus dictated by the solution of:

$$i\partial_t \psi(x, t) = \left(-\frac{1}{2}\partial_x^2 + v(x) + v_d(x, t) \right) \psi(x, t), \quad (20)$$

where $v_d(xt) = Ex \sin \omega t$, and the external potential is $v = v_L + v_R$. The density obtained from the above evolution equation is $n^{\text{ref}}(xt) = |\psi(xt)|^2$, which is the target density we wish to represent.

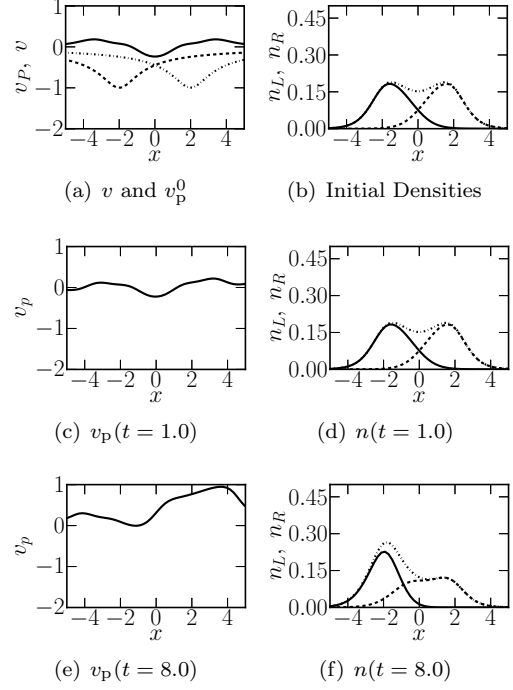


Figure 1: Snapshots of the partition potential. In a), solid line: Initial partition potential, dashed line: Left fragment external potential, dashed-dotted line: Right fragment external potential. In b), d), and f), solid lines: Left electronic density, dashed lines: Right electronic density. In d) and f) the dashed-dotted line is the total density.

The laser parameters are $\omega = 0.3$, $E_0 = 0.05$. We propagate the states of the system using the Crank-Nicholson method; time step is 0.1, box length is 20, spatial step is 0.2, and total propagation time is 10 units. The partition potential is represented in a smoothed, cubic, spline basis set with 22 knots equally spaced in the box. The initial partition potential is estimated by minimizing the error using sequential quadratic programming (other useful methods employ the density error directly [20]). To obtain the initial densities, the error functional of Eq. (17) (with the time-dependency dropped) is minimized. First the problem $(-1/2\partial_x^2 + v_{\alpha} + v_p^0)\phi_{n,\alpha} = \epsilon_{n,\alpha}\phi_{n,\alpha}$ is solved (with the finite-difference method) for both wells with some estimation of v_p^0 . Then, the density is compared with that of the system of reference in order to propose the next estimation in the iterative procedure of sequential quadratic programming; the constraints are conservation of charge and chemical potential (HOMO) equalization [12]. Figure 1.a.

shows the initial partition potential and external potentials of each well. The initial fragment densities that add up to the ground-state density of the supermolecule are displayed in Figure 1.b.

The estimation of the evolution of v_p is determined by using the step-by-step scheme proposed in Ref. [11], and the norm of Eq. (17): For example, for $\Delta t = 0.1$, the error norm can be approximated as

$$\Delta t \sum_i \{ \tilde{n}^{\text{ref}}(x_i, \Delta t) [(\partial_x e(x_i, \Delta t))^2 + (\partial_t e(x_i, \Delta t))^2] \}. \quad (21)$$

The numerical value of the above quantity depends on the value of v_p at the spline knots and at $t = \Delta t/2$. Hence, this quantity is varied until the above function is minimized and the total density of the fragments match that of the true system. The procedure is repeated similarly for the rest of the propagation. Figure 1.c. shows the partition potential at $t = 1.0$; it is localized in the intermediate region between the fragments. The fragment electronic densities (Figure 1.d) are also well localized at $t = 1.0$. Because in absence of the partition potential the fragment-densities would just be localized around their wells, the partition potential must be such that it induces the transfer of charge from the right fragment into the left fragment (Figure 1.e). However, as we note in Figure 1.f, the charge transfer in this case is represented by the spreading of the right electronic density into the left one, not by a change in the fragment populations. Two observations: i) If one were to assign a grid that is fine enough around the center of the wells and then coarser as one moves away from the wells, then to describe the density spreading, the grid would need to be time-dependent. ii) The partition potential must induce the charge transfer and act like a ‘‘spoon’’.

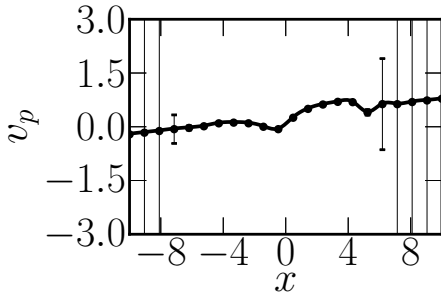


Figure 2: Error-bar plot of the partition potential at $t = 6.2$. Solid line: Interpolated optimal potential, circles: Interpolation knots.

The result of the error estimation in the partition potential at $t = 6.2$ is shown in Figure 2. As expected, in the boundary regions, the error is quite significant, and the error bars extend well beyond the plotting range. This implies that the shape of the potential in these regions is not reliable. All space-time points obeying causality are coupled. For example, variation of a single knot in the boundary affects its neighbors, introducing large gradient fluctuations. Thus, the error can spread to regions where the density is non-negligible. This can cause instabilities in the minimization procedure if a norm such as $\int d^3\mathbf{r} dt (\tilde{n}^{\text{ref}}(\mathbf{r}, t) - n(\mathbf{r}, t))^2$ is employed. For this reason we recommend the use of derivatives of the density to measure the error.

5 Variable Occupation Numbers

Let us assign variable electron-occupation numbers to the fragments. First, divide the total propagation time into blocks: $[0, \tau) \cup [\tau, 2\tau) \cup \dots \cup [(m-1)\tau, m\tau)$, where $m\tau$ is the final time of the propagation, and let

$$X_\alpha = \{ |\xi_\alpha^0\rangle, |\xi_\alpha^1\rangle, \dots, |\xi_\alpha^{m-1}\rangle \}, \quad (22)$$

be a set of instantaneous kets, in Fock space, for fragment α . At a single time $t = k\tau$, the following minimization is performed to obtain the set of kets describing the density of the fragmented molecule:

$$\begin{aligned} \{ |\xi_\alpha^k\rangle \}_{\alpha=1}^{N_{\text{frag}}} = \arg \min \left\{ \sum_\alpha \langle \psi_\alpha^k | \hat{H}_\alpha^0 | \psi_\alpha^k \rangle \text{ s.t.} \right. \\ \left. \sum_\alpha \langle \psi_\alpha^k | \hat{n}(\mathbf{r}) | \psi_\alpha^k \rangle = n(\mathbf{r}, k\tau), \forall \mathbf{r} \right\}, \quad (23) \end{aligned}$$

The occupation numbers of fragment α are formally expressed as $|\nu_{\alpha, M}(k\tau)|^2 = |\langle \xi_{\alpha, M}^k | \xi_\alpha^k \rangle|^2$. Here, $|\xi_{\alpha, M}^k\rangle$ is an optimal ket (obtained from solving the right hand side of Eq. (23)) for fragment α with M electrons. These numbers are density-functionals.

The evolution operator of fragment α is: $\hat{U}_\alpha[v_p](t_1, t_2) = \mathcal{T} \exp(-i \int_{t_0}^{t_1} ds \hat{H}_\alpha[v_p](s))$. Introduce the displaced set of kets:

$$\begin{aligned} \tilde{X}_\alpha = \{ \hat{U}_\alpha(\tau, 0) |\xi_\alpha^0\rangle, \\ \hat{U}_\alpha(2\tau, \tau) |\xi_\alpha^1\rangle, \dots, \hat{U}_\alpha(m\tau, (m-1)\tau) |\xi_\alpha^{m-1}\rangle \}. \quad (24) \end{aligned}$$

Now let us define the following dyadic product: $(X_\alpha \tilde{X}_\alpha^\dagger)(k) = |\xi_\alpha^k\rangle \langle \xi_\alpha^{k-1}|$. The symbol $X_\alpha \tilde{X}_\alpha^\dagger$ is the

set of dyadic products where the k -th component is the dyadic product between the ket at the beginning of the k -th block and the displaced ket from the $k-1$ -th block. Now, let \hat{B}_α be the TD operator:

$$\begin{aligned}\hat{B}_\alpha(t) &= (W_\tau * \ln X_\alpha \tilde{X}_\alpha^\dagger)(t) \\ &= \sum_{k=1}^m \delta(t - k\tau) \ln |\xi_\alpha^k\rangle \langle \tilde{\xi}_\alpha^{k-1}|.\end{aligned}\quad (25)$$

where W_τ is the Dirac-Comb kernel. Addition of the operator \hat{B}_α to the Hamiltonian $\hat{H}_\alpha(t)$ yields the non-Hermitian operator:

$$\hat{H}_{c,\alpha}[v_p](t) = \hat{H}_\alpha[v_p](t) + i\hat{B}_\alpha[v_p](t). \quad (26)$$

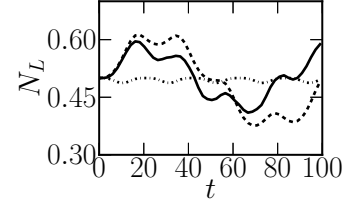
The evolution of the system is now determined by $|\psi_\alpha[v_p]\rangle$, which obeys

$$i\partial_t |\psi_\alpha[v_p](t)\rangle = \hat{H}_{c,\alpha}[v_p](t) |\psi_\alpha[v_p](t)\rangle. \quad (27)$$

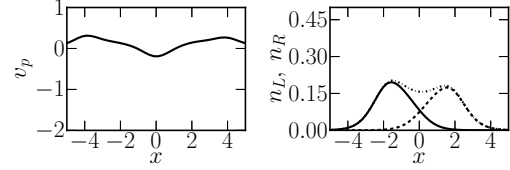
The total density is $n(\mathbf{r}t) = \sum_\alpha \langle \psi_\alpha(t) | \hat{n}(\mathbf{r}) | \psi_\alpha(t) \rangle$ and the number of particles in fragment α is $N_\alpha(t) = \langle \psi_\alpha(t) | \hat{N} | \psi_\alpha(t) \rangle$. In general, any observable, $\hat{O}(t)$, is expressed as a functional of the partition potential, $\langle \psi_\alpha[v_p](t) | \hat{O}(t) | \psi_\alpha[v_p](t) \rangle$.

Given the partition potential and occupation numbers as density-functionals, the scheme to determine the evolution of the molecule is the following: First, propagate the kets $\{|\psi_\alpha\rangle\}$ in the interval $[0, \tau)$ with fixed populations on each fragment. Then, at $t = \tau$, obtain new occupation numbers according to Eq. (23) as well as new states to propagate; continue the propagation in the block $[\tau, 2\tau)$. The procedure continues similarly for the rest of the propagation. The density of the system is then obtained as $n(\mathbf{r}, t) = \sum_\alpha \langle \psi_\alpha(t) | \hat{n}(\mathbf{r}) | \psi_\alpha(t) \rangle$. The theorem discussed in section 2 also applies in this case. Therefore, the partition potential for this scheme is uniquely determined by the TD electronic density, up to an arbitrary constant.

The partition potential is discontinuous at the relaxation nodes (points where t is an integer multiple of τ). Discontinuities in time can be eliminated by using an integral transformation that smooths the observable at the relaxation nodes. In practice, however, it is convenient to propagate the occupation numbers and gluing potential assuming that they are continuously differentiable functions of time. It can be shown, assuming that the dynamics of the occupation numbers is much slower than that of the partition potential, that the 1-1 map between the former and the density still holds. This follows from the scheme

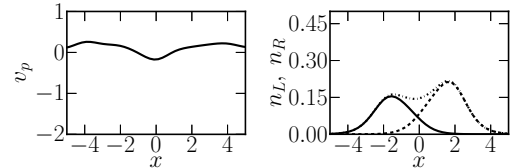


(a) N_L



(b) $v_p(t=40)$

(c) $n(t=40)$



(d) $v_p(t=70)$

(e) $n(t=70)$

Figure 3: Evolution of the fragments with TD electron populations. In a) the solid line is the result from the inversion, the dashed line is the result from the two-state approximation, and the dashed-dotted line is obtained by omitting the gluing potential: $v_G = 0$. In c) and e), solid line: n_L , dashed line: n_R , dashed-dotted: n .

we have shown here because the electronic populations are fixed in the first block, allowing us to apply the Runge-Gross theorem in such block.

A density-functional approximation to the occupation numbers is needed to apply the theory. The dynamics of the occupation numbers can be investigated using master equations, where the rate coefficients are determined by Fermi's golden rule, or transition elements that couple the fragments. Here, we illustrate a simple approach: A trial wave function to investigate the evolution of the occupation numbers is $|\eta(t)\rangle = a_L(t)|\varphi_L\rangle + a_R(t)|\varphi_R\rangle$, where $|\varphi_\alpha\rangle$ is the ground-state of the electron described only by \hat{H}_α^0 (This hamiltonian in coordinate representation is $-1/2\partial_x^2 + v_\alpha(x)$). The dynamics of electron transfer is governed by a two-component wave-function $\mathbf{a} = (a_L, a_R)^T$. We assume that the Hamiltonian coupling that relates the two fragments is of the form:

$$\hat{H}(t) = \hat{H}_f^0 + \int dx (v_G(x, 0) + v_d(x, t)) \hat{n}(x) \quad (28)$$

where $\hat{H}_f^0 = \hat{H}_L^0 \oplus \hat{H}_R^0$, is the uncoupled Hamiltonian; $\hat{H}_\alpha^0|\varphi_\beta\rangle = 0$ if $\alpha \neq \beta$. For the sake of the illustration, the gluing field is frozen, serving as a “bridge” for the charge to be transferred from one well into the other.

From the evolution equation: $i\partial_t|\eta(t)\rangle = \hat{H}(t)|\eta(t)\rangle$ we infer that the state vector, \mathbf{a} , satisfies:

$$i\partial_t\mathbf{a}(t) = \mathbf{S}^{-1}(\boldsymbol{\epsilon}_0 + \boldsymbol{\Delta}(t))\mathbf{a}(t) \quad (29)$$

where $S_{\alpha\beta} = \int dx \varphi_\alpha^*(x)\varphi_\beta(x)$, $\boldsymbol{\epsilon}_0 = \text{diag}(\epsilon_0, \epsilon_0)$, and

$$\Delta_{\alpha\beta}(t) = \int dx \varphi_\alpha^*(x)(v_G(x,0) + v_d(x,t))\varphi_\beta(x) . \quad (30)$$

The occupation numbers are obtained from the “density” of \mathbf{a} : $N_\alpha(t) = |\mathbf{a}_\alpha|^2(t) + \text{Re}(a_L^*(t)a_R(t)S_{LR})$. The last term arises from the overlap of the functions φ_L and φ_R , guaranteeing that $N_L + N_R = 1$.

The example of the previous section, summarized in Fig. 1., illustrates how the partition potential can be estimated even under a strong laser field. We now return to the example of section 4.2 and allow for variable occupations. The parameters for the propagation now are $\tau = 2$, $\Delta t = 1$, $\omega = 0.3$, $E_0 = 0.02$. Comparison of the exact time-dependency of the average number of electrons of the left fragment with the approximation described above is shown in Figure 3.a. The initial gluing potential used here is that shown in Fig. 1.a. The two-state approximation works well at short times, and displays deviations after $t = 20$. Capturing the results of the two-state approximation would be quite challenging by fixing the occupation numbers and finding the corresponding partition potential. Improvements over the two-state approximation can proceed by either refining the gluing potential (going beyond the frozen approximation) or increasing the number of states considered to couple the fragments. The first alternative has the advantage that the equations can be solved very fast. Nonetheless, for functional development, the gluing potential is also a determinant factor for the evolution of the shape of the electronic fragment-density ($\int n_\alpha/N_\alpha$).

Figure 3.b shows a snapshot of the “exact” partition potential at $t = 40$. In contrast with the results of section 3.2, the partition potential is now well localized (Figures 3.d and 3.f). This suggests that the standard methods of ground-state PDFPT can be used to estimate the partition potential through the use of the adiabatic approximation. The fragment densities also remain localized (Figure 3.c, 3.e, and 3.g). Qualitatively, the partition potential accounts

for the shape of the electronic densities of the fragments, while the occupation numbers are responsible for their height.

6 Concluding Remarks

We formulated a TDDFT for treating molecules as composed of smaller composite units. The successful application of this formulation requires approximations to the partition potential and the occupation numbers. This can be accomplished by a proper approximation to the Hamiltonians $\{\hat{H}_{c,\alpha}(t)\}$, or the auxiliary evolution equations of the electron populations in the fragments. The error analysis was also presented. It leads to a simple form of estimating the errors in the potentials. The partition potential, obtained by numerical inversion, can be uncertain in spatio-temporal regions where the density is small. However, as time increases, the error can propagate from the boundary areas into regions where the density is high.

7 Acknowledgments

We acknowledge support from the National Science Foundation CAREER program under grant No.CHE-1149968. AW also acknowledges support from the Alfred P. Sloan Foundation and the Camille Dreyfus Teacher-Scholar Awards Programs.

References

- [1] Eberhard K. U. Gross and Neepa T. Maitra. Introduction to TDDFT Fundamentals of Time-Dependent Density Functional Theory. volume 837 of *Lecture Notes in Physics*, chapter 4, pages 53–99. Springer Berlin / Heidelberg, Berlin, Heidelberg, 2012. ISBN 978-3-642-23517-7.
- [2] Erich Runge and E. K. U. Gross. Density-Functional Theory for Time-Dependent Systems. *Phys. Rev. Lett.*, 52(12):997, March 1984.
- [3] Volker Peuckert. A new approximation method for electron systems. *J. Phys. C: Solid State Physics*, 11(24):4945, 1978.
- [4] A Zangwill and Paul Soven. Resonant photoemission in barium and cerium. *Phys. Rev. Lett.*, 45(3):204, 1980.

- [5] Mark E. Casida and Tomasz A. Wesolowski. Generalization of the Kohn–Sham equations with constrained electron density formalism and its time-dependent response theory formulation. *Int. J. Quantum Chem.*, 96(6):577–588, 2004.
- [6] Chiba Mahito, Dmitri G. Fedorov, and Kazuo Kitaura. Time-dependent density functional theory based upon the fragment molecular orbital method. *J. Chem. Phys.*, 127:104108, 2007.
- [7] Johannes Neugebauer. Chromophore-specific theoretical spectroscopy: From subsystem density functional theory to mode-specific vibrational spectroscopy. *Phys. Rep.*, 489(1-3):1–87, April 2010. ISSN 03701573.
- [8] Michele Pavanello. On the subsystem formulation of linear-response time-dependent dft. *J. Chem. Phys.*, 138(20):204118, 2013.
- [9] Johannes Neugebauer. Couplings between electronic transitions in a subsystem formulation of time-dependent density functional theory. *J. Chem. Phys.*, 126(13):134116, 2007.
- [10] Andre Severo Pereira Gomes and Christoph R. Jacob. Quantum-chemical embedding methods for treating local electronic excitations in complex chemical systems. *Annu. Rep. Prog. Chem., Sect. C: Phys. Chem.*, 108(1):222–277, 2012.
- [11] Martín A Mosquera, Daniel Jensen, and Adam Wasserman. Fragment-based time-dependent density functional theory. *Phys. Rev. Lett.*, 111(2):023001, 2013.
- [12] Martín A Mosquera and Adam Wasserman. Current density partitioning in time-dependent current density functional theory. *J. Chem. Phys.*, 140(18):18A525, 2014.
- [13] Chen Huang, Florian Libisch, Qing Peng, and Emily A Carter. Time-dependent potential-functional embedding theory. *J. Chem. Phys.*, 140(12):124113, 2014.
- [14] Peter Elliott, Kieron Burke, Morrel H. Cohen, and Adam Wasserman. Partition density-functional theory. *Phys. Rev. A*, 82(2):024501, August 2010.
- [15] Martín A. Mosquera and Adam Wasserman. Partition density functional theory and its extension to the spin-polarized case. *Mol. Phys.*, 111(4):505–515, September 2013.
- [16] Morrel H. Cohen and Adam Wasserman. On Hardness and Electronegativity Equalization in Chemical Reactivity Theory. *J. Stat. Phys.*, 125(5):1121–1139, December 2006. ISSN 0022-4715.
- [17] Alberto Castro, Jan Werschnik, and Eberhard KU Gross. Controlling the dynamics of many-electron systems from first principles: a combination of optimal control and time-dependent density-functional theory. *Phys. Rev. Lett.*, 109(15):153603, 2012.
- [18] Michael Ruggenthaler and Robert van Leeuwen. Global fixed-point proof of time-dependent density-functional theory. *Europhys. Lett.*, 95(1):13001, 2011.
- [19] GAF Seber and CJ Wild. *Nonlinear Regression*. Wiley, New York, 1989.
- [20] Octavio Roncero, Alfredo Aguado, Fidel A Batista-Romero, Margarita I Bernal-Uruchurtu, and Ramón Hernández-Lamonedá. Density-difference-driven optimized embedding potential method to study the spectroscopy of br2 in water clusters. *J. Chem. Phys.*, 11(3):1155–1164, 2015.